Orbital angular momentum entanglement via fork-poling nonlinear photonic crystals

L. L. Lu, P. Xu,* M. L. Zhong, Y. F. Bai, and S. N. Zhu

National Laboratory of Solid State Microstructures, Nanjing University, Nanjing, 210093, China

*pingxu520@nju.edu.cn

Abstract: We report a compact scheme for the generation and manipulation of photon pairs entangled in the orbital angular momentum (OAM) from the fork-poling quadratic nonlinear crystal. The $\chi^{(2)}$-modulation in this crystal is designed for fulfilling a tilted quasi-phase-matching geometry to ensure the efficient generation of entangled photons as well as for transferring of topological charge of the crystal to the photon pairs. Numerical results show that the OAM of photon pair is anti-correlated and the degree of OAM entanglement can be enhanced by modulating the topological charge of crystal, which indicates a feasible extension to high-dimensional OAM entanglement. These studies suggest that the fork-poling nonlinear photonic crystal a unique platform for compact generation and manipulation of high-dimensional and high-order OAM entanglement, which may have potential applications in quantum communication, quantum cryptography and quantum remote sensing.

OCIS codes: (190.4410) Nonlinear optics, parametric processes; ((190.4390) Nonlinear optics, integrated optics;(270.4180) Multiphoton processes.

References and links

1. Y. H. Shih and C. O. Alley, "New type of Einstein-Podolsky-Rosen-Bohm experiment using pairs of light quanta produced by optical parametric down conversion," Phys. Rev. Lett. **61**, 2921–2924 (1988).
2. C. K. Hong, Z. Y. Ou, and L. Mandel, "Measurement of subpicosencond time intervals between two photons by interference," Phys. Rev. Lett. **59**, 2044–2046 (1987).
3. S. P. Walborn, S. Padua, and C. H. Monken, "Hyperentanglement-assisted Bell-state analysis," Phys. Rev. A **68**, 042313 (2003).
4. P. J. Mosley, J. S. Lundeen, B. J. Smith, P. Wasylczyk, A. B. Uren, C. Silberhorn, and I. A. Walmsley, "Heralded generation of ultrafast single photons in pure quantum states," Phys. Rev. Lett. **100**, 133601 (2008).
5. J. P. Torres, G. Molina-Terriza, and L. Torner, "The spatial shape of entangled photon states generated in non-collinear, walking parametric downconversion," J. Opt. B: Quantum Semiclass. Opt. **7**, 235–239 (2005).
6. A. Mair, A. Vaziri, G. Weihs, and A. Zeilinger, "Entanglement of the orbital angular momentum states of photons," Nature **412**, 313–316 (2001).
7. H. Di Lorenzo Pires, H. C. B. Florijn, and M. P. van Exter, "Measurement of the spiral spectrum of entangled two-photon states," Phys. Rev. Lett. **104**, 020505 (2010).
8. J. Leach, B. Jack, J. Romero, A. K. Jha, A. M. Yao, S. Franke-Arnold, D. G. Ireland, R. W. Boyd, S. M. Barnett, and M. J. Padgett, "Quantum correlations in optical angle-orbital angular momentum variables," Science **329**, 662–665 (2010).
9. V. D. Salakhutdinov, E. R. Eliel, and W. Loffler, "Full-field quantum correlations of spatially entangled photons," Phys. Rev. Lett. **108**, 173604 (2012).
10. R. Fickler, R. Lapkiewicz, W. N. Plick, M. Krenn, C. Schaeff, S. Ramelow, and A. Zeilinger, "Quantum entanglement of high angular momenta," Science **338**, 640–643 (2012).

#229006 - $15.00 USD Received 5 Dec 2014; revised 2 Jan 2015; accepted 2 Jan 2015; published 20 Jan 2015

11. M. Mclaren, T. Mhlanga, M. J. Padgett, F. S. Roux, and A. Forbes, "Self-healing of quantum entanglement after an obstruction," Nat. Commun. **5**, 3248 (2014)
12. A. C. Dada, J. Leach, G. S. Buller, M. J. Padgett, and E. Andersson, "Experimental high-dimensional two-photon entanglement and violations of generalized Bell inequalities," Nat. Phys. **7**, 677–680 (2011).
13. J. Romero, D. Giovannini, S. Franke-Arnold, S. M. Barnett, and M. J. Padgett, "Increasing the dimension in high-dimensional two-photon orbital angular momentum entanglement," Phys. Rev. A **86**, 012334 (2012).
14. L. Allen, M. W. Beijersbergen, R. J. C. Spreeuw, and J. P. Woerdman, "Orbital angular momentum of light and the transformation of Laguerre-Gaussian laser modes" Phys. Rev. A **45**, 8185–8189 (1992).
15. A. K. Jha, G. S. Agarwal, and R. W. Boyd, "Supersensitive measurement of angular displacements using entangled photons," Phys. Rev. A **83**, 053829 (2011).
16. M. M. Fejer, G. A. Magel, D. H. Jundt, and R. L. Byer, "Quasi-phase-matched second harmonic generation: tuning and tolerances," IEEE J. Quantum Electron **28**, 2631–2654 (1992).
17. J. P. Meyn, C. Laue, R. Knappe, R. Wallenstein, and M. M. Fejer, "Fabrication of periodically poled lithium tantalate for UV generation with diode lasers," Appl. Phys. B: Lasers Opt. **73**, 111-114 (2001), and references therein.
18. V. Berger, "Nonlinear photonic crystals," Phys. Rev. Lett. **81**, 4136–4139 (1998).
19. N. G. R. Broderick, G. W. Ross, H. L. Offerhaus, D. J. Richardson, and D. C. Hanna, "Hexagonally poled lithium niobate: a two-dimensional nonlinear photonic crystal," Phys. Rev. Lett. **84**, 4345–4348 (2000).
20. N. V. Bloch, K. Shemer, A. Shapira, R. Shiloh, I. Juwiler, and A. Arie, "Twisting light by nonlinear photonic crystals," Phys. Rev. Lett. **108**, 233902 (2012).
21. A. Shapira, R. Shiloh, I. Juwiler, and A. Arie, "Two dimensional nonlinear beam shaping," Opt. Lett. **37**, 2136–2138 (2012).
22. A. Shapira, I. Juwiler, and A. Arie, "Tunable nonlinear beam shaping by non-collinear interactions," Laser Photon. Rev. **7**, L25–L29 (2013).
23. H. Ishizuki and T. Taira, "Half-joule output optical-parametric oscillation by using 10-mm-thick periodically poled Mg-doped congruent $LiNbO_3$," Opt. Express **20**, 20002–20010 (2012).
24. T. Ellenbogen, N. V. Bloch, A. G. Padowicz, and A. Arie, "Nonlinear generation and manipulation of Airy beams," Nat. Photon. **3**, 395–398 (2009).
25. J. P. Torres, A. Alexandrescu, S. Carrasco, and L. Torner, "Quasi-phase-matching engineering for spatial control of entangled two-photon states," Opt. Lett. **29**, 376–378 (2004).
26. X. Q. Yu, P. Xu, Z. D. Xie, J. F. Wang, H. Y. Leng, J. S. Zhao, S. N. Zhu, and N. B. Ming, "Transforming spatial entanglement using a domain-engineering technique," Phys. Rev. Lett. **101**, 233601 (2008).
27. H. Y. Leng, X. Q. Yu, Y. X. Gong, P. Xu, Z. D. Xie, H. Jin, C. Zhang, and S. N. Zhu, "On-chip steering of entangled photons in nonlinear photonic crystals," Nat. Commun. **2**, 429 (2011).
28. T. Roger, J. J. F. Heitz, E. M. Wright, and D. Faccio, "Non-collinear interaction of photons with orbital angular momentum," Sci. Rep. **3**, 3491 (2013).
29. F. M. Miatto, H. Di Lorenzo Pires, S. M. Barnett, and M. P. van Exter, "Spatial Schmidt modes generated in parametric down-conversion," Eur. Phys. J. D **66**, 263 (2012).
30. F. M. Miatto, T. Brougham, and A. M. Yao, "Cartesian and ploar Schmidt bases for down-converted photons," Eur. Phys. J. D **66**, 183 (2012).
31. F. M. Miatto, A. M. Yao, and S. M. Barnett, "Full characterization of the quantum spiral bandwidth of entangled biphotons," Phys. Rev. A **83**, 033816 (2011).
32. B. Pors, F. Miatto, G. W't. Hooft, E. R. Eliel, and J. P. Woerdman, "High-dimensional entanglement with orbital-angular-momentum states of light," J. Opt. **13**, 064008 (2011).
33. M. Mclaren, M. Agnew, J. Leach, F. S. Roux, M. J. Padgett, R. W. Boyd, and A. Forbes, "Entangled Bessel-Gaussian beams," Opt. Express **20**, 23589–23597 (2012).

1. Introduction

Entangled photons play an important role in studying the fundamental issues of quantum mechanics, quantum information science and technology. The widely used method to generate entangled photons is spontaneous parametric down conversion (SPDC) in nonlinear crystals [1–2]. The popularity of SPDC lies on the relative simplicity of its experimental realization, and on the variety of quantum features that down-converted photons exhibit. The photon pair generated via SPDC can be entangled in polarization, frequency, space, and orbital angular momentum (OAM) [3–6]. A number of investigations on the entanglement between spatial modes carrying OAM has been discussed in the literatures owing to the extended possibilities they provide [7–13]. For example, by increasing the size of the entangled quantum system, a variety of fundamental tests [12] as well as higher-information-density coding can be performed [13].

#229006 - $15.00 USD Received 5 Dec 2014; revised 2 Jan 2015; accepted 2 Jan 2015; published 20 Jan 2015

Modes carrying OAM are most commonly described in the Laguerre-Gaussian (LG) mode set; these modes have amplitude distributions, $LG_{p,l}$, characterized as [14]

$$LG_{p,l} = \sqrt{\frac{2p!}{\pi(|l|+p)!}}\frac{1}{\omega(z)}(\frac{\sqrt{2}\rho}{\omega(z)})^{|l|}L_p^{|l|}(\frac{2\rho^2}{\omega^2(z)})\exp(-\frac{\rho^2}{\omega^2(z)})\exp(il\varphi)$$
$$\exp[\frac{ik_0r^2z}{2(z^2+z_R^2)}]\exp[-i(2p+|l|+1)tan^{-1}(\frac{z}{z_R})], \quad (1)$$

in which $\omega(z)=\omega(0)[(z^2+z_R^2)/z_R^2]^{1/2}$ with z_R being the Rayleigh range. The index l determines the OAM carried by the photon in $\hbar$ units, and p gives the number of nonaxial vortices and $2p+l$ the mode order N. $L_p^l(x)$ is the associated Laguerre polynomial. The LG modes can form a complete Hilbert space and can thus be used to represent the paraxial regime of light propagation. An important potential application of light beams carrying OAM is the generation of photon pairs with discrete multidimensional entanglement. The OAM entanglement is a quantum superposition of two-photon amplitudes over a variety of l_i and l_s.

So far, the OAM entanglement between two photons differing by $600\hbar$ has been achieved [10]. In addition to expanding the dimension of Hilbert space, the OAM entanglement can bring an increased angular resolution which is enlarged by large OAM value [10, 15] in quantum remote sensing when compared with classical methods. Therefore to engineer and manipulate the OAM entanglement becomes a pivotal task in this field. The traditional method to generate the OAM entanglement is the SPDC process, typically using the birefringence phase-matching in a nonlinear crystal. Theoretical and experimental studies have shown that the OAM is conserved during the SPDC process [6–13]. The tunable high-dimensional OAM entanglement can be achieved by tuning the phase-matching conditions [7, 13].

In this paper we propose an alternative but compact scheme for the generation and manipulation of OAM entanglement from the $\chi^{(2)}$ nonlinear photonic crystal (NPC). The NPC, as a type of artificial material with modulated quadratic susceptibility $\chi^{(2)}$, can achieve high-efficiency nonlinear interaction in a quasi-phase-matching (QPM) way or a required wavefront of the parametric wave, or for both [16–24]. The sign of $\chi^{(2)}$ in such a crystal is modulated by reversing the orientation of ferroelectric domain according to some sequence to contribute an additional "momentum" to compensate the mismatch of wavevectors among the interacting waves. Nowadays, the NPC has been utilized in quantum optics, especially in the shaping of spatial forms of entangled photons [25–27] which indicates that the study of QPM technique has entered a new regime. Here in this work through the design of quadratic susceptibility of the crystal, the NPC has a topological charge or quasi-angular momentum of its own which can be further transferred to the photon pair during the SPDC process inside it. The degree of OAM entanglement can be enhanced by increasing the crystal's topological charge. Meanwhile, some particular OAM states are also feasible and can be created with higher efficiency with respect to the widely adopted methods based on post-selecting the OAM states.

2. Two-photon state from forked-poling nonlinear photonic crystal

We consider a quadratic nonlinear photonic crystal like $LiNbO_3$ with a fork-shaped susceptibility pattern in a type 0(*ooo*) SPDC configuration coupled with collinear propagation of the signal, and idler photons. The fork-poling NPC is used for both satisfying the phase-matching requirements to ensure high conversion efficiency and encoding the spatial information. Figure 1 shows a schematic illustration of the suggested setups, the pump beam is propagating in the $x-z$ plane with a tilted angle of θ. The k-vector diagram is presented to explain the QPM scheme. The NPC can be poled following the structure function,

$$\chi^{(2)}(x,\varphi) = d_{22}sgn(\cos[2\pi x/\Lambda + l_c\varphi]), \quad (2)$$

#229006 - $15.00 USD Received 5 Dec 2014; revised 2 Jan 2015; accepted 2 Jan 2015; published 20 Jan 2015

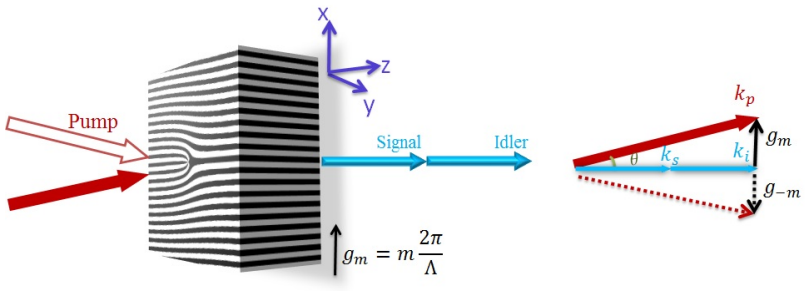

Fig. 1. Schematic diagram of the fork-shaped nonlinear photonic crystal and the momentum conservation of the tilted SPDC.

which indicates the nonlinear coefficient d_{22} is utilized and its sign changes when the domain is inverted with the poling period Λ. $\varphi = \tan^{-1}(y/x)$ is the azimuthal angle and l_c is the topological charge of the crystal which can have an integer or fractional value. The Fourier expansion of this binary modulation function is $d_{22}\sum_n F(g_n)e^{ig_n x + il_c\varphi}$, where $g_n = n\frac{2\pi}{\Lambda}$ (n=±1, ±2,...) represents the nth-order reciprocal vector and $F(g_n) = \frac{2}{\pi n}\sin(\pi n D)$ corresponds to its Fourier coefficient. D is called duty cycle, defined as a ratio of inverted-region width to the QPM period Λ. Optimum structure for efficient QPM device means perfectly vertical penetration of inversion from $+z$ to $-z$ surface with $D = 0.5$. Moreover, the smaller order reciprocal vector is, the higher the SPDC conversion efficiency will be. The interaction Hamilton inside the NPC can be written as

$$\hat{H} = \varepsilon_0 \int d\vec{r}\chi^{(2)}\hat{E}_p^{(+)}\hat{E}_s^{(-)}\hat{E}_i^{(-)} + h.c. \tag{3}$$

$\hat{E}^{(-)}$ and $\hat{E}^{(+)}$ are the negative- and positive- frequency parts of the electric field. H.c. means the Hermitian conjugate. We will take the pump as Gaussian TEM_{00} and treat it classically for simplicity. The beam waist ω_0 is located at the center of the crystal. At the beam waist ($z = 0$), it can be expressed in the scalar approximation

$$\hat{E}_p = C_0 \exp(-\frac{(x\cos\theta - z\sin\theta)^2 + y^2}{\omega_0^2})\exp[i(k_p\cos\theta z + k_p\sin\theta x - \omega_p t)], \tag{4}$$

where C_0 is normalization constant. Whereas the produced signal and idler photons are treated quantum mechanically, the negative parts of the field operators are

$$E_j^{(-)} = A_j \int d\omega_j \int d\vec{q}_j \exp[-i(\vec{q}_j\cdot\vec{\rho} + k_{jz}z - \omega_j t)]\hat{a}_j^+(\vec{q}_j), \tag{5}$$

where $\hat{a}_j^+(\vec{q}_j)$ $(j = s, i)$ is the creation operator, and A_j is the normalization coefficient. Therefore the interaction Hamilton can be written as

$$\begin{aligned} H \quad \propto \quad & \int d\omega_s \int d\omega_i \exp[i(\omega_s + \omega_i - \omega_p)t] \int d\vec{q}_s d\vec{q}_i \int d\vec{\rho} dz \\ & \times \exp[i(k_p\cos\theta - k_{sz} - k_{iz})z]\exp[i(g_n + k_p\sin\theta)\rho\cos\varphi]\exp(il_c\varphi) \\ & \times \exp(-\frac{(\rho\cos\varphi\cos\theta - z\sin\theta)^2 + (\rho\sin\varphi)^2}{\omega_0^2})\exp[-i(\vec{q}_s + \vec{q}_i)\vec{\rho}]\hat{a}_s^+(\vec{q}_s)\hat{a}_i^+(\vec{q}_i), \end{aligned} \tag{6}$$

in which, under the assumption of a monochromatic signal and idler photons, the longitudinal components of wave vectors through Taylor expansions are $k_{jz} = k_j - q_j^2/2k_j$. Hence the

#229006 - $15.00 USD Received 5 Dec 2014; revised 2 Jan 2015; accepted 2 Jan 2015; published 20 Jan 2015

entangled photons are generated under a tilted QPM condition,

$$k_p \sin\theta + n\frac{2\pi}{\Lambda} = 0, \tag{7}$$

$$k_p \cos\theta - k_s - k_i = 0, \tag{8}$$

where k_p, k_s, k_i represent the wave vectors of pump, signal, idler, respectively. We take the SPDC process of 780 nm (n_o=2.15585)$\rightarrow$ 1560 nm (n_o=2.119)+1560 nm (n_o=2.119) at $T = 27^0C$ in a PPLT crystal as the example. SPDC sources at such wavelengths have wide applications in long-distance fiber-based quantum information processing. From Eqs. (7) and (8), one can get $\theta = 10.6^o$ and the transversal periodicity of NPC is $\Lambda = 5.88\ \mu m$, which ensures efficient entangled photons generation with the third-order reciprocal vector $g_3 = 3*(2\pi)/\Lambda$. The crystal length L=0.5 *mm* and the beam waist ω_0=2 *mm*. Then we can neglect any *z*-variation of the pump field envelopes based on the fact that the Rayleigh range of the pump field is much larger than the medium length. The shift of the beam waist during the propagation is 0.12 mm which is negligible as compared to $\omega_0 = 2$ *mm* due to the non-collinear length ($L_{nc} = \omega_0/\sin\theta$) is much larger than the crystal length ($L \ll L_{nc}$) in this case. Thus the effect of the non-collinear geometry is negligible and the coefficient $cos(\theta)$ (≈ 0.983) can be taken as 1 during the calculation [5, 28]. Therefore, the wave function evaluated from first-order perturbation theory can be written as

$$\Psi \propto \int d\vec{q}_s d\vec{q}_i Sinc[\frac{\Delta k_z}{2}L] F(\vec{q}_s,\vec{q}_i)\hat{a}_s^+(\vec{q}_s)\hat{a}_i^+(\vec{q}_i)|vac>_s |vac>_i, \tag{9}$$

where

$$\begin{aligned} F(\vec{q}_s,\vec{q}_i) &= \int d\vec{\rho}\exp(il_c\varphi)\exp(-\frac{\rho^2}{\omega_0^2})\exp[-i\Delta k_x\rho\cos\varphi]\exp[-i\Delta k_y\rho\sin\varphi] \\ &= \int \rho d\rho \exp(-\frac{\rho^2}{\omega_0^2})\exp[il_c(\phi+\pi/2)]J_{l_c}(-\rho\sqrt{\Delta k_x^2+\Delta k_y^2}) \\ &= F(\Delta k)\exp[il_c\phi], \end{aligned} \tag{10}$$

with $\Delta k_x = q_{sx} + q_{ix}$, $\Delta k_y = q_{sy} + q_{iy}$, $\Delta k^2 = \Delta k_x^2 + \Delta k_y^2$, $\tan\phi = \Delta k_y/\Delta k_x$ and J_l are Bessel functions of the first kind. We have used the Jacobi-Anger expansion $exp[ix\sin\theta] = \sum_m J_m(x)e^{im\theta}$ in the middle line. Furthermore, one can decompose the quantum state Ψ in the base of the eigenstaes of the OAM operator as $\Psi \propto \sum_{l_s p_s}\sum_{l_i p_i} C_{p_s p_i}^{l_s l_i}|l_s,p_s;l_i,p_i\rangle$, with $|l_j,p_j\rangle = \int d\vec{q}_j LG(\vec{q}_j)a^+(\vec{q}_j)|0\rangle$ (j=s,i), yields the amplitudes

$$C_{p_s p_i}^{l_s l_i} \propto \int d\vec{q}_s d\vec{q}_i Sinc[\frac{\Delta k_z}{2}L] F(\Delta k)\exp[il_c\phi] LG_{l_s p_s}^*(\vec{q}_s) LG_{l_i p_i}^*(\vec{q}_i), \tag{11}$$

where the mode function $LG_{lp}(\vec{q})$ is the normalized LG modes in *k* space.

For simplicity, we assume the pump, signal, and idler beam have same beamwidth. Then numerical evaluation will suggest that the terms in the *sinc* function is negligible due to the thin crystal. Eq. (11) can also be written in the spatial space as

$$C_{p_s p_i}^{l_s l_i} \propto \int d\vec{\rho}\exp[-\frac{\rho^2}{\omega_0^2}]\exp[il_c\varphi] LG_{l_s p_s}^*(\vec{\rho}) LG_{l_i p_i}^*(\vec{\rho}). \tag{12}$$

$LG_{p,l}(\vec{\rho})$ is the amplitude distribution at the beam waist. The integral over the azimuthal coordinate is

$$\int_0^{2\pi} d\varphi \exp[i(l_c - l_s - l_i)\varphi] = 2\pi\delta_{l_c, l_s+l_i}, \tag{13}$$

#229006 - $15.00 USD Received 5 Dec 2014; revised 2 Jan 2015; accepted 2 Jan 2015; published 20 Jan 2015

which clearly enforces the OAM conservation: $l_c = l_s + l_i$. The integral over the radial coordinate gives

$$C_{p_s p_i}^{l_s l_i} \propto \delta_{l_c, l_s+l_i} (\frac{2}{3})^{\xi+1} \sqrt{p_s! p_i! (p_s+|l_s|)! (p_i+|l_i|)!} \sum_{i=0}^{p_s} \sum_{j=0}^{p_i} (\frac{-2}{3})^{i+j} \times \frac{(\xi+i+j)!}{(p_s-i)!(|l_s+i|)! i! (p_i-j)!(|l_i+j|)! j!}, \tag{14}$$

where $\xi = (|l_s| + |l_i|)/2$. The weights of the quantum superposition can be represented as $P_{p_s,p_i}^{l_s,l_i} = |C_{p_s,p_i}^{l_s,l_i}|^2$, which indicates the joint detection probability for finding one photon in the signal mode (l_s, p_s) and the other one in the idler mode (l_i, p_i).

3. The general quasi-phase-matching condition for OAM entanglement

It is worth noting that in the above discussions the signal and idler photons are designed to emit perpendicularly with the x-y plane, which requires a large transverse reciprocal vector to fulfill the transverse phase-matching of the SPDC process, therefore the high-order QPM geometry is involved. This greatly reduces the efficiency of SPDC process, thus resulting a lower flux of photon pairs. Here we propose a modified but more general QPM geometry which requires a smaller reciprocal vector, i.e. a larger poling period so that the first-order QPM will be feasible in experiment. The modified QPM diagram is presented in the inset of Fig. 2. Here the signal and idler beams are still collinear but has a crossing angle θ with z-axis. α represents the angle between parametric beams and pump beam. The proposed general QPM geometry can introduce both phase-matching and encoded information on the same crystal axis and offer a major improvement in conversion efficiency of the SPDC process. The transverse wave vectors can be written as $\vec{q}_s$ and $\vec{q}_i$, with $k_{jl} = \sqrt{k_j^2 - q_j^2} \approx k_j - q_j^2/2k_j$. q_j contains the in-plane and out-of-plane projections, written as $q_{j\parallel}$ and $q_{j\perp}$ respectively, with $q = \sqrt{q_{j\parallel}^2 + q_{j\perp}^2}$. Hence we have

$$\vec{k}_j \cdot \vec{r}_j = (k_{jl} \sin\theta - q_{j\parallel} \cos\theta) x + q_{j\perp} y + (k_{jl} \cos\theta + q_{j\parallel} \sin\theta) z, \tag{15}$$

and the phase mismatch along x, y, and z directions can be written as

$$\Delta k_x = \Delta k_{x0} + (\frac{q_s^2}{2k_s} + \frac{q_i^2}{2k_i}) \sin\theta + (q_{s\parallel} + q_{i\parallel}) \cos\theta, \tag{16}$$

$$\Delta k_y = q_{sy} + q_{iy}, \tag{17}$$

and

$$\Delta k_z = \Delta k_{z0} + (\frac{q_s^2}{2k_s} + \frac{q_i^2}{2k_i}) \cos\theta - (q_{s\parallel} + q_{i\parallel}) \sin\theta, \tag{18}$$

with

$$\Delta k_{x0} = k_p \sin(\theta+\alpha) - (k_s + k_i) \sin\theta - \frac{2\pi}{\Lambda} = 0 \tag{19}$$

$$\Delta k_{z0} = k_p \cos(\theta+\alpha) - (k_s + k_i) \cos\theta = 0. \tag{20}$$

Equations. (19) and (20) represent the QPM conditions in the NPC. According to these conditions, we then draw the poling period as a function of the angle (θ). It it notable that the poling period increases with θ. Therefore, it is possible to achieve the first-order QPM by tilting the parametric beams. Compared with the third-order QPM process with aforementioned QPM geometry when $\theta = 0$, the SPDC efficiency can be improved by 9 times due to the increment of the Fourier coefficient $F(g_n)$. For an example, we can choose $\theta = 8.6^o$ (the corresponding

#229006 - $15.00 USD Received 5 Dec 2014; revised 2 Jan 2015; accepted 2 Jan 2015; published 20 Jan 2015

$\alpha = 5^o$) and this corresponds to the poling period of $\Lambda = 4.1\mu m$, which is technically feasible in experiments [17, 22]. This is different from previous schemes [20–21], where the full vectorial phase-matching condition was not fulfilled although their periods varied from 10 to 30 μm. The disadvantage of the partial phase-matching scheme is the resultant low nonlinear conversion efficiency, yielding the nonlinear Raman-Nath pattern.

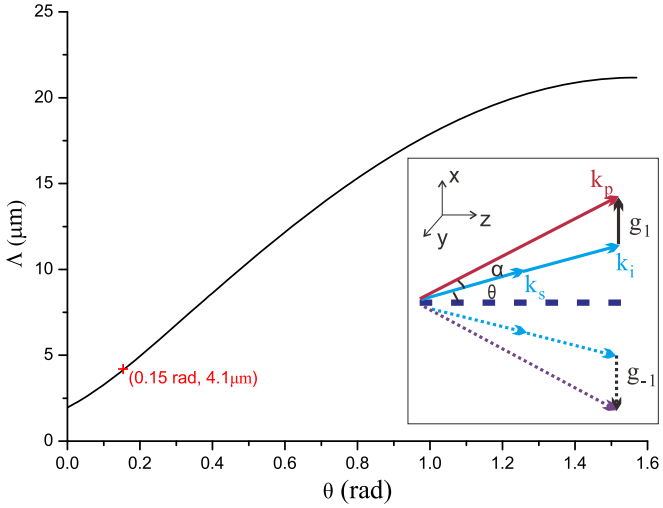

Fig. 2. The poling period, whose reciprocal vector is the first-order, as a function of θ. The parameter we used in the discussion is annotated. Inset graph shows the $k-$ vector diagram.

Based on Fig. 2, the larger poling period can be approached when further increasing the tilted angle of parametric beams. However, this may cause the nonconservation of OAM [7] when the approximation condition ($L_{nc} \gg L$) is not satisfied any more. So for this modified QPM condition should be designed one hand to relax the poling technique and on the other hand to enforce the OAM conservation. The annotated parameters in Fig. 2 are appropriate. In this case, the term $\vec{q}_{s(i)}$ in Eq. (11) can be written as $q'_{s(i)x}\hat{x'} + q_{s(i)y}\hat{y}$, with $q'_{s(i)x} = \frac{q^2_{s(i)}}{2k_{s(i)}}\sin\theta + q_{s(i)\|}\cos\theta$ in the coordinate shown in the inset of Fig. 2 (Here $\hat{x'}$ is along the propagation direction of the parametric beams). Then the term $\Delta k_x = q'_{sx} + q'_{ix}$, and following the same derivation carried out above, one can also get the OAM conservation law denoted by Eqs. (12) and (13). It deserves to emphasize that for the tilted QPM scheme, the parametric beams are generated collinearly but noncollinearly with the pump, which offers the natural separation with the pump and gets rid of the dichroic element. The SPDC efficiency can be further increased by using thick QPM crystals. $Mg-$doped $LiNbO_3$ accompanied by a reduced coercive field to invert the polarization and a suppressed photo-refractive damage is a candidate of the thick high-energy QPM device. The $10-mm$ thick $Mg-$doped $LiNbO_3$, realized in experiments, results in a great increment of the nonlinear conversion efficiency [23]. A much larger beam waist and smaller incident angle of the pump beam are needed in this case.

#229006 - $15.00 USD Received 5 Dec 2014; revised 2 Jan 2015; accepted 2 Jan 2015; published 20 Jan 2015

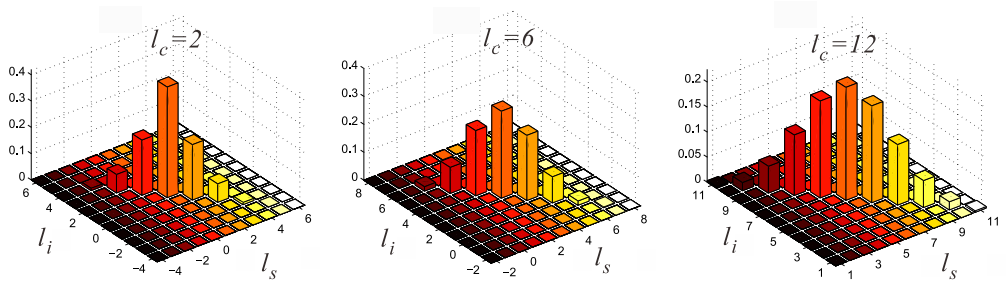

Fig. 3. Correlations between l_s and l_i for different values of l_c, $l_c = 2$, $l_c = 6$, $l_c = 12$, with $p_s = p_i = 0$.

4. Characterizations on the degree of OAM entanglement

In most applications that make use of the OAM of photons, one may project the state into a subspace of the complete Hilbert space that describes the mode function of the photon. This implies considering only a fraction of the mode space. In Fig. 3 we plot the coincidence probabilities as a function of l_s and l_i for different values of l_c with p_s=p_i=0. As it shows, the OAM of photon pair is always anti-correlated under different l_c, i.e. the larger l_s corresponds to a smaller l_i mode. This is consistent with the conversation law of $l_c = l_s + l_i$. The correlation reaches its maximum at $l_s = l_i = l_c/2$. The physical origin is that maximum overlap between the pump and the signal/idler modes, and hence maximum coincidence amplitudes, occurs at $l_c/2$. Moreover, as the value of l_c increases, the quantum spiral bandwidth gets larger, which indicates an increment of the usable number of entangled optical modes.

To extract the amount of entanglement involved in Ψ, one may resort to the Schmidt decomposition, $|\Psi>_{AB} = \sum_n \sqrt{\lambda_n}|\phi_n>_A |\varphi_n>_B$, where $|\phi_n>_A$, $|\varphi_n>_B$ are the Schmidt modes defined by eigenvectors of the reduced density matrices for the signal and idler photons, respectively, and $\sqrt{\lambda_n}$ are the corresponding eigenvalues. Once the Schmidt coefficients are obtained, one can obtain $K = 1/\sum_n \lambda_n^2$, which can be interpreted as a measure of the effective dimensionality of the system. Since we are interested in the OAM entanglement, we can perform the Schmidt decomposition in the azimuthal modes, $|\Psi>= \sum_l C_l |l> |l_c - l>$, which are automatically Schmidt modes [29–33]. We can also quantify the entanglement by I-concurrence, defined as $C(\Psi) = \sqrt{2(1-\sum_l C_l^2)}$.

In Fig. 4, we show the Schmidt number (K) and I-concurrence (C) as a function of l_c for $p_s = p_i = 0$. Obviously, the degree of OAM entanglement increases with l_c. This is consistent with Fig. 2 since larger extension of the number of modes are involved for larger l_c. This shows the OAM entanglement can be engineered by designing the structure of NPC. We also consider what happens to the Schmidt number when the mode numbers p are not zero. As shown in Fig. 5, we find that for $p_s = p_i > 0$, K decreases dramatically when $l_c \neq 0$ which is quite different from the case of $p_s = p_i = 0$. In this case, there exists big contrast of Schmidt number. We choose $l_c = 0$ and $l_c = 20$ while $p_s = p_i = 8$ to plot the OAM correlation as the insets of Fig. 5. For the low K case, only several finite modes are involved. This can be useful for the engineering of high order OAM entanglement by setting large l_c, which can significantly improve the sensitivity of angular resolution in remote sensing [10]. While for the high K case, the OAM correlation is involved with a number of modes, indicating a way to engineer high-dimensional OAM entangled state. Moreover, very high-dimensional Hilbert spaces become accessible if we make use of the full spatial entanglement, i.e. hybrid azimuthal-radial quantum correlations, by properly chosen detection-mode waist [9].

#229006 - $15.00 USD Received 5 Dec 2014; revised 2 Jan 2015; accepted 2 Jan 2015; published 20 Jan 2015

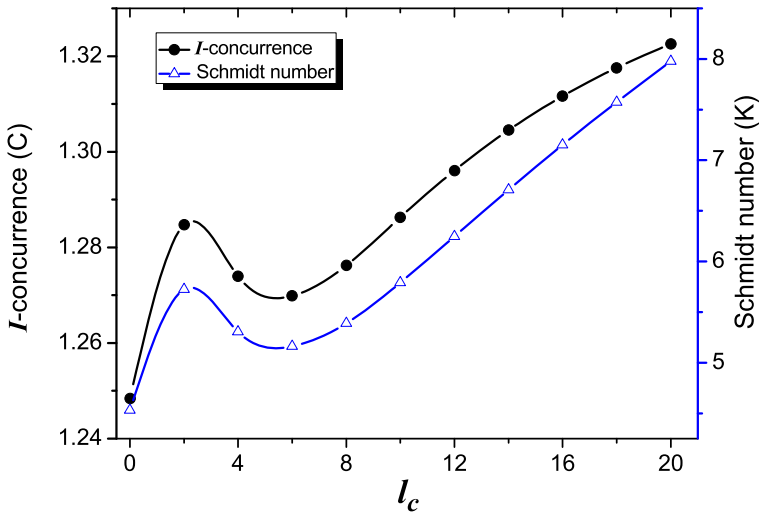

Fig. 4. The Schmidt number (K) and I-concurrence (C) as a function of l_c for $p_s = p_i = 0$. The smooth fit lines are to guide the eye.

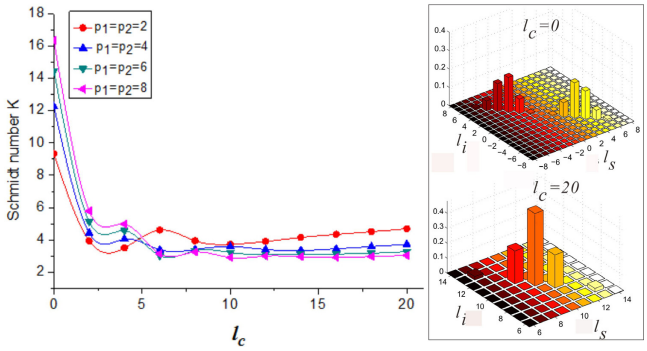

Fig. 5. The Schmidt number K as a function of l_c for different values of the radial indices p_s (p_i). Inset, the correlation distribution between l_s and l_i for two different cases: $l_c = 0$ and $l_c = 20$ with $p_s = p_i = 8$. The smooth fit lines are to guide the eye.

5. Conclusion

In conclusion, we have investigated a compact scheme for generating and manipulating OAM entanglement from the fork-poling quadratic nonlinear crystal under the condition of a tilted QPM geometry is fulfilled. The first-order QPM is realizable to ensure high nonlinear conversion efficiency. The total OAM is conserved through translating the crystal's topological information into the photons interacting in this crystal. Our results show that the fork-poling NPCs with high topological charge can directly lead to high-order OAM entanglement with high efficiency, which can significantly improve the sensitivity of angular resolution in remote sensing.

#229006 - $15.00 USD Received 5 Dec 2014; revised 2 Jan 2015; accepted 2 Jan 2015; published 20 Jan 2015

Modulation of the topological charge of fork-poling NPCs can obviously increase the amount of accessible entangled OAM modes, i.e. the degree of OAM entanglement. A growing body of theoretical work calls for entanglement of quantum systems of higher dimensions. This opens the door to generate high entanglement under various experimental conditions. Hence this compact QPM device could give rise to new applications in the fields of quantum communication, quantum cryptography and quantum remote sensing.

Acknowledgments

It is a pleasure to thank Dr. F. S. Roux and Dr. Hassan Hassanabadi for stimulating discussions. This work was supported by the State Key Program for Basic Research of China (No. 2012CB921802 and No. 2011CBA00205), the National Natural Science Foundations of China (Nos. 10409066, 91121001 and 11021403) and the Project Funded by the Priority Academic Program Development of Jiangsu Higher Education Institutions (PAPD).

#229006 - $15.00 USD Received 5 Dec 2014; revised 2 Jan 2015; accepted 2 Jan 2015; published 20 Jan 2015